Hindawi Publishing Corporation
Journal of Nanomaterials
Volume 2012, Article ID 708648, 5 pages
doi:10.1155/2012/708648

Research Article

Dilute Magnetic Semiconductor Cu_2FeSnS_4 Nanocrystals with a Novel Zincblende Structure

Xiaolu Liang,[1,2] Xianhua Wei,[1] and Daocheng Pan[2]

[1] *State Key Laboratory Cultivation Base for Nonmetal Composites and Functional Materials, Southwest University of Science and Technology, Mianyang 621010, China*
[2] *State Key Laboratory of Rare Earth Resource Utilization, Changchun Institute of Applied Chemistry, Chinese Academy of Sciences, 5625 Renmin Street, Changchun 130022, China*

Correspondence should be addressed to Xianhua Wei, weisansao@yahoo.com.cn and Daocheng Pan, pan@ciac.jl.cn

Received 15 February 2012; Revised 13 April 2012; Accepted 17 April 2012

Academic Editor: Weichang Hao

Diluted magnetic semiconductor Cu_2FeSnS_4 nanocrystals with a novel zincblende structure have been successfully synthesized by a hot-injection approach. Cu^+, Fe^{2+}, and Sn^{4+} ions occupy the same position in the zincblende unit cell, and their occupancy possibilities are 1/2, 1/4, and 1/4, respectively. The nanocrystals were characterized by means of X-ray diffraction (XRD), transmission electron microscopy (TEM), selected area electron diffraction (SAED), energy-dispersive spectroscopy (EDS), and UV-vis-NIR absorption spectroscopy. The nanocrystals have an average size of 7.5 nm and a band gap of 1.1 eV and show a weak ferromagnetic behavior at low temperature.

1. Introduction

During the past three decades, transition metal ion-doped diluted magnetic semiconductors (DMSs) have attracted great interest because of their outstanding the optical, electronic, and magnetic properties [1–5]. Fe^{2+}, Ni^{2+}, Mn^{2+}, and Co^{2+} are commonly used as intentional impurities and incorporated in group II-VI and III-V semiconductors; ZnO, ZnS, ZnSe, CdS, CdSe, and GaN are the frequently used host materials [6–8]. However, the magnetic ion concentration in these doped DMS nanocrystals is generally less than 2 mol% [9–13]. It is well known that the magnetic properties of DMSs are strongly dependent on the magnetic ion concentration. Nonetheless, a high magnetic ion concentration is detrimental to the magnetic properties for binary DMSs due to the strong antiferromagnetic (AFM) interactions between nearest-neighbor-doping ions [14].

The quaternary Cu_2FeSnS_4 with a high magnetic ion concentration is being considered as an ideal material for avoiding large AFM exchange interactions [14]. However, Cu_2FeSnS_4 usually crystallizes in a stannite structure (space group *I-42 m*, no. 121), and Cu^+, Fe^{2+}, and Sn^{4+} cations have a fixed position in the stannite unit cell [15]. In the previously reports, quaternary Cu_2FeSnS_4 magnetic semiconductor with a stannite structure exhibited an antiferromagnetic behavior with a Néel temperature (T_N) of 6~8 K [15–17]. To the best of our knowledge, there are no reports on the synthesis of Cu_2FeSnS_4 nanocrystals with a zincblende structure in the literature. In this paper, we adopted a hot-injection approach to synthesize quaternary Cu_2FeSnS_4 nanocrystals with a metastable zincblende structure. In zincblende structure, all of cations have a random distribution instead of ordered distribution, which may lead peculiar magnetic properties by controlling both metal distribution and metal-metal distance. The magnetic properties of zincblende Cu_2FeSnS_4 nanocrystals were investigated by a superconducting quantum interference device (SQUID).

2. Experimental

2.1. Chemicals. $CuCl_2 \cdot 2H_2O$, $FeCl_3 \cdot 6H_2O$, $SnCl_4 \cdot 5H_2O$, sulfur powder (99.999%), thiourea, and oleylamine (OM, 80% ~ 90%) were purchased from Aladdin Inc. All chemicals were used as received.

2.2. Preparation of Sulfur Precursors. 1.0 M S/OM solution was prepared by dissolving 0.64 g (20 mmol) of sulfur powder in 20.0 mL of OM at 120°C.

2.3. Synthesis of Zincblende Cu_2FeSnS_4 Nanocrystals. In a typical synthesis, 17.0 mg (0.1 mmol) of $CuCl_2 \cdot 2H_2O$, 17.0 mg (0.05 mmol) of $SnCl_4 \cdot 5H_2O$, 13.5 mg (0.05 mmol) of $FeCl_3 \cdot 6H_2O$, and 5.0 mL of OM were added to a 50 mL three-neck flask, and the reaction mixture was heated to 120°C. The inside of the flask was degassed by a vacuum pump for 10 min, and argon gas was charged. This procedure was repeated three times. Then the temperature was increased to 270°C, and 0.5 mL of S/OM solution was injected into the flask. After 30 min, the crude solution was cooled to 60°C and then precipitated with 30 mL of ethanol. Finally, the nanocrystals were dispensed in toluene.

2.4. Characterization. X-ray diffraction (XRD) patterns were recorded by a Bruker D8 FOUCS X-ray diffractometer using Cu Kα radiation, and the accelerating voltage and current were 40 kV and 40 mA, respectively. UV-vis-NIR absorption spectrum was measured by Shimadzu UV-3600. Transmission electron microscopy (TEM) and selected area electron diffraction (SAED) images were taken on a FEI Tecnai G2 F20 with an accelerating voltage of 200 kV. Energy disperse X-ray spectroscopy (EDS) spectrum was obtained by using a scanning electron microscope (Hitachi S-4800) equipped with a Bruker AXS XFlash detector 4010. The magnetization of Cu_2FeSnS_4 nanocrystals was obtained by SQUID (MPMS-XL-7, Quantum Design, Ltd.) between 2 and 100 K using zero-field-cooled (ZFC) and field-cooling (FC) procedures in an applied field of 50 Oe.

3. Results and Discussion

In contrast to the tetragonal stannite structure, the space symmetry of zincblende structure significantly decreases by the random arrangement of Cu^+, Fe^{2+}, and Sn^{4+} cations in the cubic zincblende unit cell of Cu_2FeSnS_4. As shown in the inset of Figure 1, the zincblende unit cell of Cu_2FeSnS_4 is completely the same as that of ZnS (space group *F*-43 m, no. 216). Note that only Zn^{2+} position is replaced by 1/2 Cu^+, 1/4 Fe^{2+}, and 1/4 Sn^{4+}. Figure 1 shows the XRD pattern for as-synthesized Cu_2FeSnS_4 nanocrystals. Obviously, our XRD pattern did not match those reported in the literature [15–17] and the standard JCPDS card database (stannite structure, JCPDS no. 44-1476). We therefore simulated the diffraction pattern for zincblende Cu_2FeSnS_4 and compared it with the experimental pattern. The simulated and experimental patterns match very well, signifying that these nanocrystals possess a zincblende structure with a space group *F-43 m* and unit cell parameter $a = 5.429$ Å. In addition, the zincblende structure of Cu_2FeSnS_4 nanocrystals can be further confirmed by SAED image Figure 2(b). It should be noted that the lattice parameters of zincblende Cu_2FeSnS_4 nanocrystals measured from SAED images are very close to those calculated from the XRD patterns.

Low-resolution TEM image of zincblende Cu_2FeSnS_4 nanocrystals is shown in Figure 2(c). The Cu_2FeSnS_4 nanocrystals are nearly spherical in shape and have the average diameter of 7.5 nm. In addition, the nanocrystals exhibit a very narrow size distribution and have a standard

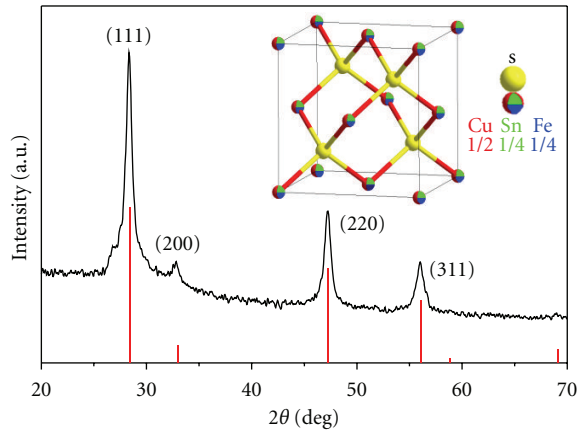

Figure 1: The simulated (red line) and experimental (black line) XRD patterns of Cu_2FeSnS_4 nanocrystals with a zincblende structure; the inset is the unit cell of zincblende Cu_2FeSnS_4.

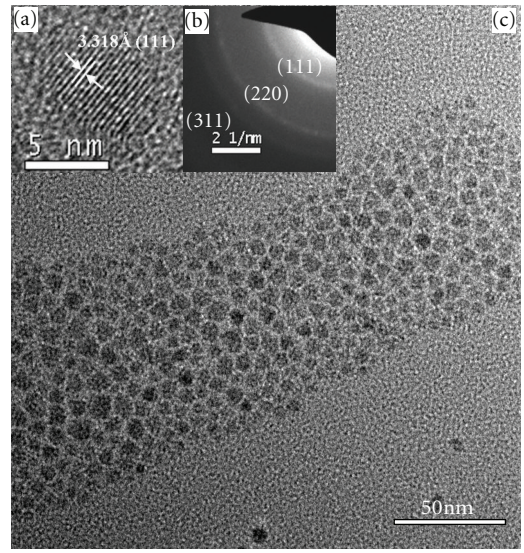

Figure 2: TEM (a and c) and SAED (b) images of Cu_2FeSnS_4 nanocrystals.

deviation of 7.4%. The high-resolution TEM image clearly revealed the continuous lattice fringes, and the calculated *d* spacing corresponding to (111) plane is 3.138 Å, which is in good agreement with that value determined by XRD pattern (3.136 Å) or SAED image (3.140 Å).

Figure 3(a) displays UV-vis-NIR absorption spectrum of as-synthesized Cu_2FeSnS_4 nanocrystals. We calculated the optical band gap (*Eg*) by extrapolating the linear portion of the absorption spectrum to $h\nu$ axis, and the calculated optical band gaps for Cu_2FeSnS_4 nanocrystals are around 1.1 eV. As demonstrated in Figure 3(b), the chemical composition of the nanocrystals is Cu_2FeSnS_4.The molar ratio of Cu/Fe/Sn/S is close to 2 : 1 : 1 : 4, which is well consistent with stoichiometric composition of Cu_2FeSnS_4.

The magnetic properties of Cu_2FeSnS_4 nanocrystals were characterized by a SQUID magnetometer. As shown in Figure 4(a), a clear separation between the ZFC and FC curves is observed at low temperature region which indicates

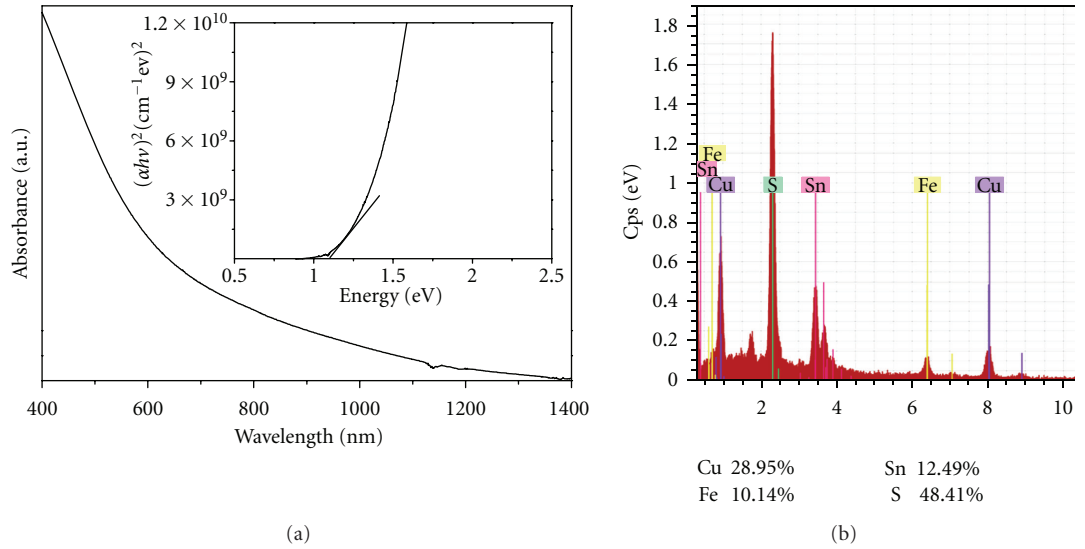

Figure 3: UV-vis-NIR absorption (a) and EDS (b) spectra of Cu_2FeSnS_4 nanocrystals.

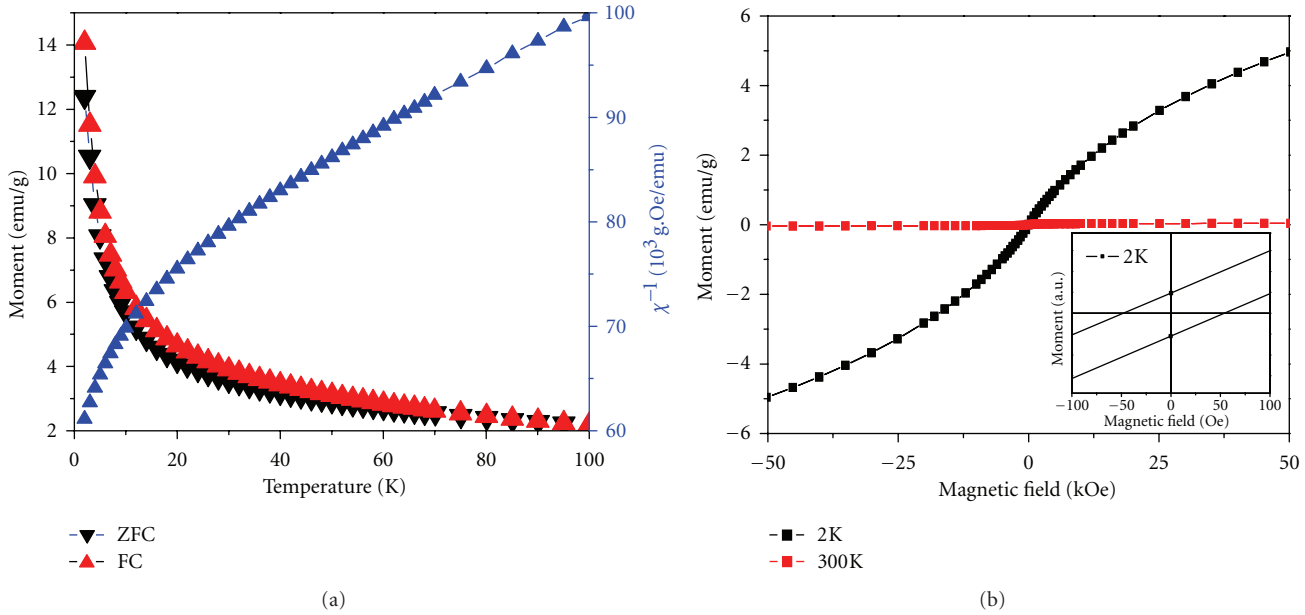

Figure 4: (a) Temperature dependence of the magnetization for Cu_2FeSnS_4 nanocrystals. (b) The field dependence of the magnetization for Cu_2FeSnS_4 nanocrystals at 2 k and 300 k; inset: the magnification of the hysteresis loop at 2 K.

the absence of a magnetic ordering transition. The plot of $\chi^{(-1)-T}$ (blue line in Figure 4(a)) indicates classical Curie-Weiss behavior of this sample at high temperature region. The magnetic susceptibility, $\chi(T)$, at the high-temperature limit can be represented by the Curie-Weiss law, $\chi(T) = C/(T - \Theta)$, where C is the Curie constant, T is the temperature in Kelvin, and Θ is the Curie temperature. The isothermal magnetization curves of Cu_2FeSnS_4 nanocrystals at 2 k and 300 k in magnetic fields up to ±50 kOe are shown in Figure 4(b). The "s" shape hysteresis loop at 2 K is shown in the inset of Figure 4(b), with a coercive force of 56 Oe and relatively large residual magnetization. It can be concluded that these Cu_2FeSnS_4 nanocrystals exhibit ferromagnetic behavior at this temperature. The hysteresis loop obtained at 300 K does not show hysteresis behavior and is weakly field dependent and linear, indicating that the nanocrystals become a paramagnetic material at 300 K. Note that the stannite Cu_2FeSnS_4 usually exhibited an antiferromagnetic behavior in the literatures [15–17]. It is well known that the unit cell parameter is 2.91 Å in iron which shows ferromagnetic behavior. In the stannite Cu_2FeSnS_4, the interaction Fe-Fe could be super-exchange interaction with the aid of nonmagnetic ions due to the large nearest distance of Fe-Fe (5.45 Å). However, the nearest distance of Fe-Fe is only 3.86 Å in the zincblende Cu_2FeSnS_4 nanocrystals, and the electron clouds overlap of Fe-Fe is more larger than that

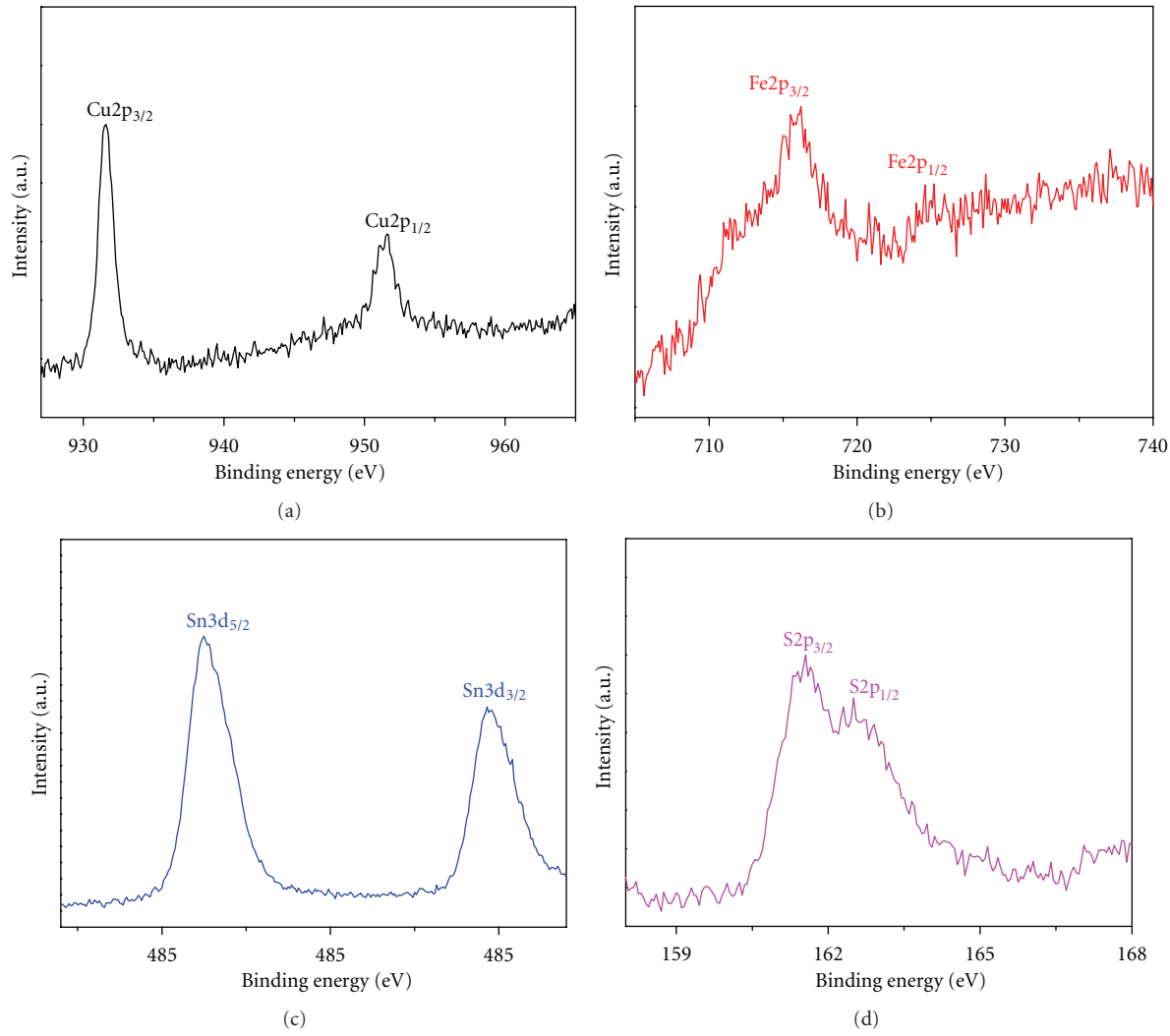

FIGURE 5: The X-ray photoelectron spectroscopy (XPS) spectra of as-synthesized Cu_2FeSnS_4 nanocrystals; (a) Cu2p; (b) Fe2p; (c) Sn3d; (d) S2p.

of stannite Cu_2FeSnS_4, enabling the exchange interaction at low temperature. As a result, Cu_2FeSnS_4 nanocrystals with a zincblende structure exhibit a ferromagnetic behavior.

In addition, X-ray photoelectron spectroscopy (XPS) was applied to determine the chemical composition and valence states of Cu_2FeSnS_4 nanocrystals. In Figure 5(a), the Cu 2p core splits into 2p3/2 (931.6 eV) and 2p1/2 (951.6 eV) peaks, which are characteristic of Cu^+. Two peaks of Fe2p and Sn3d, located at 716.0 eV and 725.7 eV, 486.4 eV and 494.7 eV, suggesting that the valence states of Fe and Sn ions in the nanocrystals are +2 and +4, respectively.

4. Conclusion

In summary, dilute magnetic semiconductor Cu_2FeSnS_4 nanocrystals with a novel zincblende structure have been successfully synthesized. The optical and magnetic properties were characterized, and the nanocrystals have a band gap of 1.1 eV and exhibited a ferromagnetic behavior at low temperature. The ferromagnetic properties may be attributed to the novel zincblende structure; that is, Cu^+, Fe^{2+}, and Sn^{4+} ions occupy the same site in the unit cell and have a random distribution. Moreover, these dispersible and low-cost DMS nanocrystals have a high potential for thin film solar cells, spintronics, magnetic switching, magnetic recording, and Li-ion batteries.

Acknowledgments

This work was supported by the National Natural Science Foundation of China (Grant nos. 21071142 and 51172229), the Fund for Creative Research Groups (Grant no. 20921002), and the Natural Science Foundation for Young Scientists of Jilin Province (20100105).

References

[1] D. J. Norris, A. L. Efros, and S. C. Erwin, "Doped nanocrystals," *Science*, vol. 319, no. 5871, pp. 1776–1779, 2008.

[2] D. J. Norris, N. Yao, F. T. Charnock, and T. A. Kennedy, "High-quality manganese-doped ZnSe nanocrystals," *Nano Letters*, vol. 1, no. 1, pp. 3–7, 2001.

[3] J. Zheng, X. Yuan, M. Ikezawa et al., "Efficient photoluminescence of Mn^{2+} ions in MnS/ZnS core/shell quantum dots," *Journal of Physical Chemistry C*, vol. 113, no. 39, pp. 16969–16974, 2009.

[4] Y. Zhang, C. Gan, J. Muhammad, D. Battaglia, X. Peng, and M. Xiao, "Enhanced fluorescence intermittency in Mn-doped single ZnSe quantum dots," *Journal of Physical Chemistry C*, vol. 112, no. 51, pp. 20200–20205, 2008.

[5] H. Kim, M. Achermann, L. P. Balet, J. A. Hollingsworth, and V. I. Klimov, "Synthesis and characterization of Co/CdSe core/shell nanocomposites: bifunctional magnetic-optical nanocrystals," *Journal of the American Chemical Society*, vol. 127, no. 2, pp. 544–546, 2005.

[6] J. K. Furdyna, "Diluted magnetic semiconductors," *Journal of Applied Physics*, vol. 64, no. 4, pp. R29–R64, 1988.

[7] N. Pradhan, D. M. Battaglia, Y. Liu, and X. Peng, "Efficient, stable, small, and water-soluble doped ZnSe nanocrystal emitters as non-cadmium biomedical labels," *Nano Letters*, vol. 7, no. 2, pp. 312–317, 2007.

[8] I. Sarkar, M. K. Sanyal, S. Kar et al., "Ferromagnetism in zinc sulfide nanocrystals: dependence on manganese concentration," *Physical Review B*, vol. 75, no. 22, Article ID 224409, 2007.

[9] M. L. Reed, M. K. Ritums, H. H. Stadelmaier et al., "Room temperature magnetic (Ga,Mn)N: a new material for spin electronic devices," *Materials Letters*, vol. 51, no. 6, pp. 500–503, 2001.

[10] Y. M. Kim, M. Yoon, I. W. Park, Y. J. Park, and J. H. Lyou, "Synthesis and magnetic properties of $Zn_{1-x}Mn_xO$ films prepared by the sol-gel method," *Solid State Communications*, vol. 129, no. 3, pp. 175–178, 2004.

[11] Z. Deng, L. Tong, M. Flores et al., "High-quality manganese-doped zinc sulfide quantum rods with tunable dual-color and multiphoton emissions," *Journal of the American Chemical Society*, vol. 133, no. 14, pp. 5389–5396, 2011.

[12] Y. W. Jun, J. H. Lee, J. S. Choi, and J. Cheon, "Symmetry-controlled colloidal nanocrystals: nonhydrolytic chemical synthesis and shape determining parameters," *Journal of Physical Chemistry B*, vol. 109, no. 31, pp. 14795–14806, 2005.

[13] K. M. Hanif, R. W. Meulenberg, and G. F. Strouse, "Magnetic ordering in doped $Cd_{1-x}Co_xSe$ diluted magnetic quantum dots," *Journal of the American Chemical Society*, vol. 124, no. 38, pp. 11495–11502, 2002.

[14] T. Fries, Y. Shapira, F. Palacio et al., "Magnetic ordering of the antiferromagnet Cu_2MnSnS_4 from magnetization and neutron-scattering measurements," *Physical Review B*, vol. 56, no. 9, pp. 5424–5431, 1997.

[15] A. Caneschi, C. Cipriani, F. Di Benedetto, and R. Sessoli, "Characterisation of the antiferromagnetic transition of Cu_2FeSnS_4 the synthetic analogue of stannite," *Physics and Chemistry of Minerals*, vol. 31, no. 3, pp. 190–193, 2004.

[16] G. P. Bernardini, D. Borrini, A. Caneschi et al., "EPR and SQUID magnetometry study of Cu_2FeSnS_4 (stannite) and Cu_2ZnSnS_4 (kesterite)," *Physics and Chemistry of Minerals*, vol. 27, no. 7, pp. 453–461, 2000.

[17] U. Ganiel, E. Hermon, and S. Shtrikman, "Studies of magnetic odering in Cu_2FeSnS_4 by Mossbauer-spectroscopy," *Journal of Physics and Chemistry of Solids*, vol. 33, pp. 1873–1878, 1972.